Human Molecular Genetics, 2011, Vol. 20, No. 24 **4891–4902**
doi:10.1093/hmg/ddr427
Advance Access published on September 14, 2011

Autophagy is increased in laminin α2 chain-deficient muscle and its inhibition improves muscle morphology in a mouse model of MDC1A

Virginie Carmignac[1,*], Martina Svensson[1], Zandra Körner[1], Linda Elowsson[1], Cintia Matsumura[1], Kinga I. Gawlik[1], Valerie Allamand[2,3,4,5] and Madeleine Durbeej[1]

[1]Muscle Biology Unit, Department of Experimental Medical Science, Lund University, Sweden, [2]UPMC Université Paris 06, IFR14, Paris, France, [3]CNRS, UMR7215, Paris, France, [4]Inserm, U974, Paris, France and [5]Institut de Myologie, Paris, France

Received June 14, 2011; Revised August 22, 2011; Accepted September 13, 2011

Congenital muscular dystrophy caused by laminin α2 chain deficiency (also known as MDC1A) is a severe and incapacitating disease, characterized by massive muscle wasting. The ubiquitin-proteasome system plays a major role in muscle wasting and we recently demonstrated that increased proteasomal activity is a feature of MDC1A. The autophagy-lysosome pathway is the other major system involved in degradation of proteins and organelles within the muscle cell. However, it remains to be determined if the autophagy-lysosome pathway is dysregulated in muscular dystrophies, including MDC1A. Using the *dy^{3K}/dy^{3K}* mouse model of laminin α2 chain deficiency and MDC1A patient muscle, we show here that expression of autophagy-related genes is upregulated in laminin α2 chain-deficient muscle. Moreover, we found that autophagy inhibition significantly improves the dystrophic *dy^{3K}/dy^{3K}* phenotype. In particular, we show that systemic injection of 3-methyladenine (3-MA) reduces muscle fibrosis, atrophy, apoptosis and increases muscle regeneration and muscle mass. Importantly, lifespan and locomotive behavior were also greatly improved. These findings indicate that enhanced autophagic activity is pathogenic and that autophagy inhibition holds a promising therapeutic potential in the treatment of MDC1A.

INTRODUCTION

Macroautophagy (hereafter referred to as autophagy or autophagocytosis) is a multi-step catabolic process involving the sequestration of bulk cytoplasm, long-lived proteins and cellular organelles in autophagosomes, which are subsequently fused with lysosomes, and their content is digested by lysosomal hydrolases (1,2). Autophagy is generally activated by conditions of nutrient or growth factor deprivation as well as endoplasmic reticulum stress. In addition, autophagy has been associated with a number of physiological processes, including development, differentiation or pathologies like neurodegenerative diseases, lysosomal storage diseases, infection and cancer (1,3). However, it is not clear if defects in autophagy are linked to muscular dystrophy. Furthermore, the role and regulation of the autophagic pathway in skeletal muscle is still largely unknown, but it is generally believed that excessive autophagy activation contributes to muscle loss during different catabolic conditions (4). Interestingly, inhibition of the autophagic flow may also result in muscle atrophy (5). In yeast, autophagy is controlled by >30 autophagy-related genes and many of them have mammalian orthologues (6). Notably, through inhibition of Akt, FoxO3 controls the transcription of several autophagy-related genes (e.g. *LC3*, *Bnip3, Gabarapl1* and *Vps34*) and therefore parts of the autophagic–lysosomal pathway during muscle atrophy (7–9).

Recently, it was demonstrated that autophagy activation is impaired in collagen VI-deficient muscular dystrophy and that its reactivation ameliorated the dystrophic phenotype in a mouse model of the disease (10). Another type of congenital muscular dystrophy is MDC1A (OMIM #607855), which is caused by autosomal recessive mutations in the human

*To whom correspondence should be addressed at: Muscle Biology Unit, Department of Experimental Medical Science, BMC B12, Lund University, 221 84 Lund, Sweden. Tel: +46 462220816; Fax: +46 462220855; Email: virginie.carmignac@med.lu.se

LAMA2 gene, encoding the α2 subunit of the basement membrane protein laminin-211. Classical MDC1A is characterized by severe generalized muscle weakness, joint contractures and peripheral neuropathy. Around 30% of the patients die within their first decade of life (11,12). The generated null mutant dy^{3K}/dy^{3K} mouse model for laminin α2 chain deficiency recapitulates human disease and presents severe muscular dystrophy as well as peripheral neuropathy. Newborn dy^{3K}/dy^{3K}mice are indistinguishable from their normal littermates but at postnatal day 14, their growth retardation and muscle wasting become apparent. By 3 weeks of age, the dy^{3K}/dy^{3K} mice are severely dystrophic and they die between 3 and 4 weeks of age (13,14). Histological features of laminin α2 chain-deficient muscle include degeneration/regeneration cycles, fiber size variability, increased apoptosis and marked connective tissue proliferation. Also, skeletal muscle atrophy is a prevalent feature of MDC1A (11,12,15).

Besides the autophagy–lysosome pathway, the ubiquitin–proteasome pathway also plays a key role in protein degradation in muscle cells and hence in regulation of muscle mass (4). In fact, we recently demonstrated increased expression of ubiquitin–proteasome-related components in laminin α2 chain-deficient muscle and that proteasome inhibition with MG-132 partially improves muscle and increases the lifespan of dy^{3K}/dy^{3K} mice (16). Furthermore, apoptosis has been considered an attractive target for therapeutic intervention in MDC1A, since there is an inappropriate induction of apoptosis in laminin α2 chain-deficient muscle (17,18). Indeed, its inhibition by genetic or pharmacological therapy ameliorated several pathological symptoms in the dy^{W}/dy^{W} mouse model of MDC1A (19–22). However, neither anti-apoptosis therapy nor proteasome inhibition resulted in complete recovery and therefore, new targets for potential pharmacological intervention should be explored.

Since enhanced proteasome activity appears to be a feature of laminin α2 chain-deficient muscle (16), we hypothesized that also autophagy is increased in MDC1A (rather than impaired as in collagen VI muscular dystrophy). Here, we show that expression of autophagy-related genes is definitely upregulated in laminin α2 chain-deficient muscle and that inhibition of the autophagy process significantly improves the dystrophic phenotype in the dy^{3K}/dy^{3K} mouse model.

RESULTS

Increased expression of autophagy-related genes in laminin α2 chain-deficient muscle

To determine whether the activity of the autophagy-lysosome pathway is increased in laminin α2 chain-deficient muscle, we first analyzed the expression of members of this pathway in dy^{3K}/dy^{3K} animals. In particular, we analyzed several genes that are controlled by the transcription factor FoxO3 (7–9), whose expression is increased ∼2-fold in 3.5-week-old dy^{3K}/dy^{3K} animals (16). We detected significantly increased mRNA levels of the microtubule-associated protein-1 light chain 3B (LC3B) and the LC3 interacting protein p62 in quadriceps muscle from 3.5-week-old dy^{3K}/dy^{3K} mice (Fig. 1A). LC3B is one of the three (human) LC3 isoforms that undergo post-translational modifications during autophagy. The presence of LC3 in autophagosomes and the conversion of LC3 to the lower migrating form LC3II have been used as indicators of autophagy (23,24). By immunofluorescence analysis, we detected accumulated LC3B in dy^{3K}/dy^{3K} quadriceps muscle fibers (Fig. 1B) and western blot analysis revealed an approximate 2-fold increase in LC3BII expression in dy^{3K}/dy^{3K} quadriceps muscle (Fig. 1C). Similarly, we noted enhanced transcript levels of *Bnip3* and *Bnip3l* (encoding BH3-only proteins) and of autophagosome membrane markers *Gabarapl1*, *Beclin* and *Vps34* [a class III phosphoinositide 3 kinase (PI3K)] as well as the cysteine protease *Atg4B* in dy^{3K}/dy^{3K} quadriceps muscle (Fig. 1A). Also, Vps34 protein expression was increased ∼2-fold in dy^{3K}/dy^{3K} quadriceps muscle (Fig. 1C). Finally, mRNA expression of lysosomal markers *Cathepsin L* and *Lamp2a* was significantly increased in dy^{3K}/dy^{3K} quadriceps muscle (Fig. 1A). In contrast, the expression levels of *Bnip3*, *Bnip3l*, *p62*, *LC3B*, *Gabarapl1*, *Vps34*, *Beclin*, *Cathepsin L* and *Lamp2a* mRNAs were not augmented in quadriceps muscle from 7-day-old dy^{3K}/dy^{3K} mice (Supplementary Material, Fig. S1). At this age, the dy^{3K}/dy^{3K} muscles appear morphologically normal (13).

To determine whether enhanced expression of autophagy-related genes is also seen in human laminin α2 chain-deficient muscle, we analyzed primary myoblasts and myotubes from a control and a laminin α2 chain-deficient patient. Increased protein expression of LC3BII, Vps34, Cathepsin L and Beclin (other proteins were not analyzed) was noted in MDC1A myotubes but not in corresponding myoblasts (Fig. 1D). Moreover, by immunofluorescence analysis, we detected accumulated LC3B in muscle biopsies obtained from two different MDC1A patients with complete laminin α2 chain deficiency (Fig. 1E and data not shown).

We next assessed quadriceps muscles from 5-week-old dy^{3K}δE3 mice. These laminin α2 chain-deficient mice overexpress a truncated laminin α1 chain devoid of the dystroglycan binding site, whereas the integrin binding site remains intact. Consequently, dy^{3K}δE3 limb muscles are dystrophic (although less affected compared with dy^{3K}/dy^{3K} muscles), whereas the diaphragm muscle is spared (25). Interestingly, the expression of the autophagy-related genes was not altered in dy^{3K}δE3 quadriceps muscles (Fig. 1F). These data indicate that the laminin α2 chain receptor dystroglycan may not be entangled with the downstream autophagic machinery. Dystroglycan is a member of the dystrophin–glycoprotein complex and mutations in several of its components lead to various forms of muscular dystrophy (26). To investigate whether autophagy is modified when dystrophin is absent and other members of the dystrophin–glycoprotein complex are reduced, we quantified the expression level of autophagy-related genes in quadriceps muscle from *mdx* mice (a Duchenne muscular dystrophy mouse model). We found no major modification in the expression of *Bnip3l*, *p62*, *LC3B, Gabarapl1*, *Beclin*, *Vps34* and *Atg4B* mRNAs in 5-week- or 3-month-old mice. Only *Bnip3* and *Cathepsin L* transcript levels were enhanced in both 5-week- and 3-month-old *mdx* muscles. Also, *Lamp2a* mRNA expression was augmented in 3-month-old *mdx* muscle (Supplementary Material, Fig. S2). Together, these data indicate that increased autophagy may not be a general feature of muscular dystrophy.

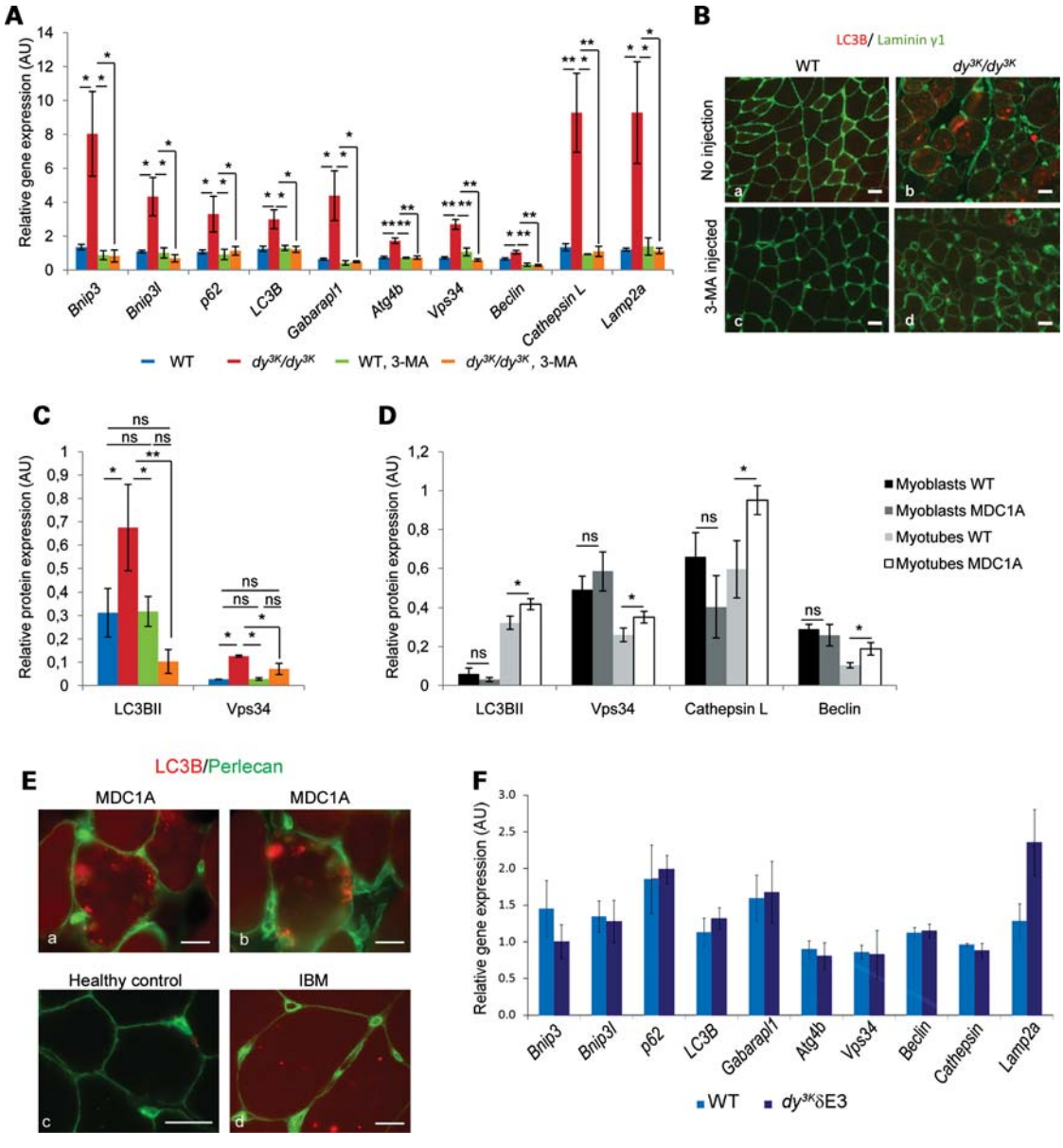

Figure 1. Autophagy is increased in skeletal muscle from dy^{3K}/dy^{3K} mice. (**A**) Relative amounts of *Bnip, Bnip3l, p62, LC3B*, *Gabarapl1*, *Atg4b*, *Vps34, Beclin, Cathepsin L* and *Lamp2a* mRNAs in quadriceps muscle from 3.5-week-old wild-type, dy^{3K}/dy^{3K} mice and from 4.5-week-old 3-MA-injected wild-type and dy^{3K}/dy^{3K} mice ($n = 6$ for each group). The *GAPDH* gene expression served as a reference. Non-significant variations are not labeled. (**B,** left panel) Co-immunostaining on cross-sections of quadriceps muscle from non-injected wild-type (a, $n = 5$) and dy^{3K}/dy^{3K} (b, $n = 5$) mice and 3-MA injected wild-type (c, $n = 6$) and dy^{3K}/dy^{3K} (d and e, $n = 6$) mice. LC3B (in red) is present in autophagosomes and laminin γ1 chain (in green) serves as delineating fiber boundaries. Bar = 40 μm. (**C**) Densitometry analysis of LC3B and Vps34 western blot analysis in quadriceps muscle from wild-type and dy^{3K}/dy^{3K} mice (3.5-week-old; $n = 6$ per group). Results are expressed in arbitrary units (AU). Labeling of tubulin served as internal loading control. (**D**) Densitometric analysis of LC3B, Vps34, Cathepsin L and Beclin-1 in human primary myoblasts and myotubes from a control and a laminin α2 chain-deficient patient. Data represent the mean of four different culture wells and are expressed in arbitrary units (AU). (**E**) Co-immunostainings on cross-sections of muscle biopsies from patients with MDC1A and inclusion-body myositis (IBM) and from a healthy control. LC3B (in red) was detected with two different antibodies in serial sections of MDC1A muscle (a and b). IBM muscle was used as a positive control for LC3B accumulation (d), whereas little LC3B staining was seen in the healthy control (c). (**F**) Relative amounts of *Bnip, Bnip3l, p62, LC3B*, *Gabarapl1*, *Atg4b*, *Vps34, Beclin, Cathepsin L* and *Lamp2a* mRNAs in 5-week-old wild-type and dy^{3K}δE3 mice ($n = 3$ for each group). The *GAPDH* gene expression served as a reference. $^{*}P < 0.05$; $^{**}P < 0.001$.

Systemic injection of 3-methyladenine restores autophagic gene expression in laminin α2 chain-deficient muscle

Since the autophagy-lysosome pathway system seemed to be overactive in dy^{3K}/dy^{3K} muscle, we envisaged that the inhibition of the autophagy pathway could improve muscle morphology and function. Thus, we administered the widely used autophagy inhibitor 3-methyladenine (3-MA), a class III PI3K inhibitor that inhibits Vps34 activity and autophagosome formation (27), into the peritoneum of 2.5-week-old dy^{3K}/dy^{3K} mice. At this age, the dy^{3K}/dy^{3K} mice are distinguishable from their littermates. We repeated the injection at

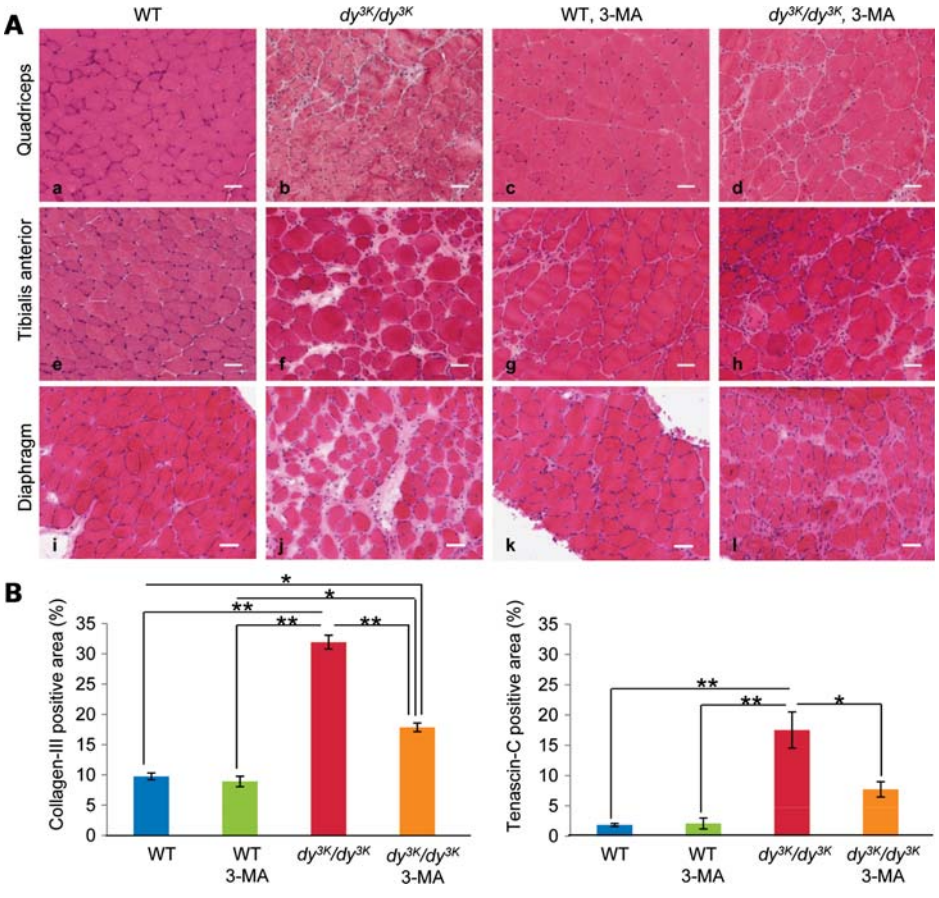

Figure 2. Muscle morphology is improved and fibrosis is reduced in skeletal muscle with systemic injection of 3-MA. (**A**) Hematoxylin–eosin staining of cross-sections of quadriceps (a–d), tibialis anterior (e–h) and diaphragm (i–l) muscles from wild-type (a, e, i), non-injected dy^{3K}/dy^{3K} (b, f, j), 3-MA-injected wild-type and dy^{3K}/dy^{3K} mice at 2.5 and 3.5 weeks of age (c, d, g, h, k, l, respectively). Fourteen days later, muscles were isolated and stained. (**B**) Densitometric quantification of fibrosis in quadriceps muscle from 3-MA-injected wild-type and dy^{3K}/dy^{3K} mice ($n = 6$ for each genotype) and non-injected dy^{3K}/dy^{3K} ($n = 7$) and wild-type mice ($n = 9$). (Left panel) Collagen III-positive labeling per total area of the section. (Right panel) Tenascin-C-positive labeling per total area of the cross-section. $^{*}P < 0.05$; $^{**}P < 0.001$.

3.5 weeks of age. We have previously shown that the median survival of dy^{3K}/dy^{3K} mice is around 22 days and most, if not all, dy^{3K}/dy^{3K} are dead by 4 weeks of age (16). We analyzed mice and muscles 14 days post-injection (a time point when dy^{3K}/dy^{3K} mice should be dead). Notably, we found that the systemic injection of 3-MA restored the expression of the autophagy-related genes to the basal level of the wild-type (Fig. 1A–C).

Systemic injection of 3-MA improves muscle morphology in laminin α2 chain-deficient muscle

Remarkably, the 3-MA injections also resulted in considerably improved muscle morphology. We first evaluated the main histological hallmarks of the dystrophic process (pathological fibrosis and decreased muscle fiber diameter) by morphometric measurements. Collagen III expression, which previously has been shown to be increased in dy^{3K}/dy^{3K} muscle (16), was reduced in quadriceps muscle of 3-MA-injected dy^{3K}/dy^{3K} mice (Fig. 2B). To further confirm the reduction in fibrosis in 3-MA-treated animals, we analyzed tenascin-C expression. Tenascin-C is only expressed at the myotendinous junctions in normal muscle, but it has been demonstrated to be highly expressed in fibrotic lesions of dy^{3K}/dy^{3K} muscle (16,28). Notably, tenascin-C expression was reduced in quadriceps muscle of 3-MA-injected mice compared with non-injected dy^{3K}/dy^{3K} mice (Fig. 2B). Also, expression of collagen III and tenascin-C was significantly reduced in tibialis anterior and diaphragm muscles of 3-MA-injected mice (Supplementary Material, Fig. S3 and data not shown).

In addition, we investigated the expression of laminin α4 and β2 chains in 3-MA-treated dy^{3K}/dy^{3K} mice. It has previously been shown that the expression of laminin α4 chain is increased at the dy^{3K}/dy^{3K} sarcolemma, whereas the laminin β2 chain expression is reduced (28,29). Expression of both proteins was near normal in quadriceps muscle of 3-MA-injected dy^{3K}/dy^{3K} mice (Supplementary Material, Fig. S4).

It is well established that the average fiber diameter is significantly reduced in dy^{3K}/dy^{3K} muscle (16,25,30). Notably, the average fiber diameter was increased upon 3-MA injection, and fiber size distribution in quadriceps muscle was significantly shifted towards larger fibers for both wild-type and dy^{3K}/dy^{3K} injected animals (Fig. 3A and B). We observed that 40% of the dy^{3K}/dy^{3K} quadriceps fibers had a diameter inferior to 20 μm, whereas the number was ∼18% in wild-type

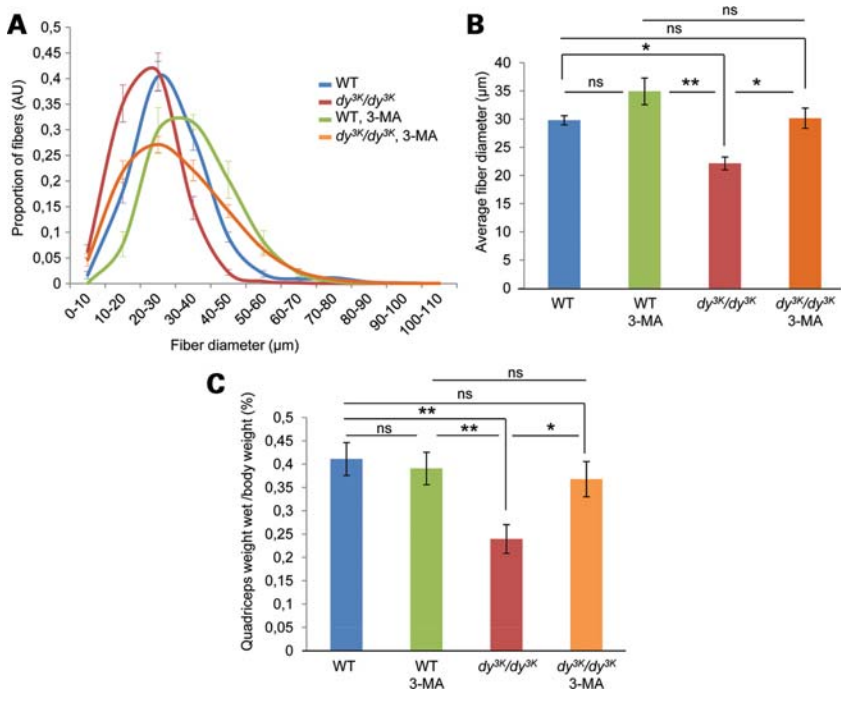

Figure 3. Atrophy is prevented in quadriceps muscle from 3-MA-treated dy^{3K}/dy^{3K} mice. (**A**) Determination of fiber diameter repartition (in percentage of total number of fibers) in 3-MA injected (green and orange) and non-injected (blue and red) wild-type and dy^{3K}/dy^{3K} mice, respectively. A significant difference exists between the curves ($P < 0.0001$). (**B**) Average of fiber diameter in µm. (**C**) Proportion (in percentage) of quadriceps muscle wet weight per body weight (wild-type, $n = 5$; dy^{3K}/dy^{3K}, $n = 4$; injected mice, $n = 5$). $^{*}P < 0.05$; $^{**}P < 0.001$.

and 22% in dy^{3K}/dy^{3K} injected animals. Furthermore, the ratio of quadriceps muscle wet weight per body weight was normalized in 3-MA-injected dy^{3K}/dy^{3K} mice, compared with age-matched non-injected dy^{3K}/dy^{3K} mice (Fig. 3C).

Systemic injection of 3-MA stimulates muscle regeneration in laminin α2 chain-deficient muscle

The proportion of fibers with centrally located nuclei is one of the main features of the degeneration–regeneration process. The number of cells with centrally located nuclei was slightly but significantly elevated in quadriceps muscle of 3-MA-injected dy^{3K}/dy^{3K} mice (Fig. 4A). We additionally performed immunofluorescence experiments analyzing the expression of regeneration markers embryonic myosin heavy chain (eMHC, a specific marker of newly regenerated fibers) and MyoD1 (present in activated satellite cells and myoblasts). Indeed, the proportion of fibers expressing eMHC significantly increased with the 3-MA injection of dy^{3K}/dy^{3K} mice (Fig. 4B). Also, the amount of MyoD1-positive nuclei was increased, indicating an improved regenerative capacity in 3-MA-injected dy^{3K}/dy^{3K} mice (Fig. 4C).

Apoptosis is decreased after systemic injection of 3-MA

As apoptosis contributes to the disease progression, we analyzed the apoptosis rate occurring in skeletal muscle of systemically injected mice. As previously described, the number of caspase-3-positive fibers (containing caspase-3 and pro-caspase-3 proteins) in dy^{3K}/dy^{3K} mice was significantly increased when compared with controls (16). Forty-eight hours after the 3-MA injection, we were able to find caspase-3-positive fibers in the same proportion as in non-injected dy^{3K}/dy^{3K} mice (data not shown), suggesting that 3-MA did not enhance apoptosis. However, 14 days after injection, the proportion of caspase-3-positive fibers was significantly decreased in 3-MA-injected dy^{3K}/dy^{3K} quadriceps muscle (Fig. 5A and B). These results were further confirmed using the terminal deoxynucleotidyl transferase dUTP nick end labeling (TUNEL) enzymatic labeling assay. While there was significantly more TUNEL-positive myonuclei in dy^{3K}/dy^{3K} quadriceps muscle (16), we found that the proportion of TUNEL-positive myonuclei was significantly reduced in 3-MA-treated dy^{3K}/dy^{3K} animals (Fig. 5C).

Systemic injection of 3-MA restores Akt phosphorylation

We have recently demonstrated that Akt phosphorylation on both threonine 308 and serine 473 is diminished in dy^{3K}/dy^{3K} quadriceps muscle, whereas the total level of Akt is unchanged (16). To investigate whether Akt activity was restored in 3-MA injected dy^{3K}/dy^{3K} mice, we euthanized mice 48 h and 14 days after injection and learned that Akt phosphorylation on both sites was reconstituted to wild-type levels at both time points (Fig. 6A and B).

Systemic injection of 3-MA increases survival and locomotive behavior, but does not significantly improve peripheral neuropathy

Dy^{3K}/dy^{3K} mice were significantly less active in an open field test (16). Remarkably, 3-MA-injected dy^{3K}/dy^{3K} mice displayed

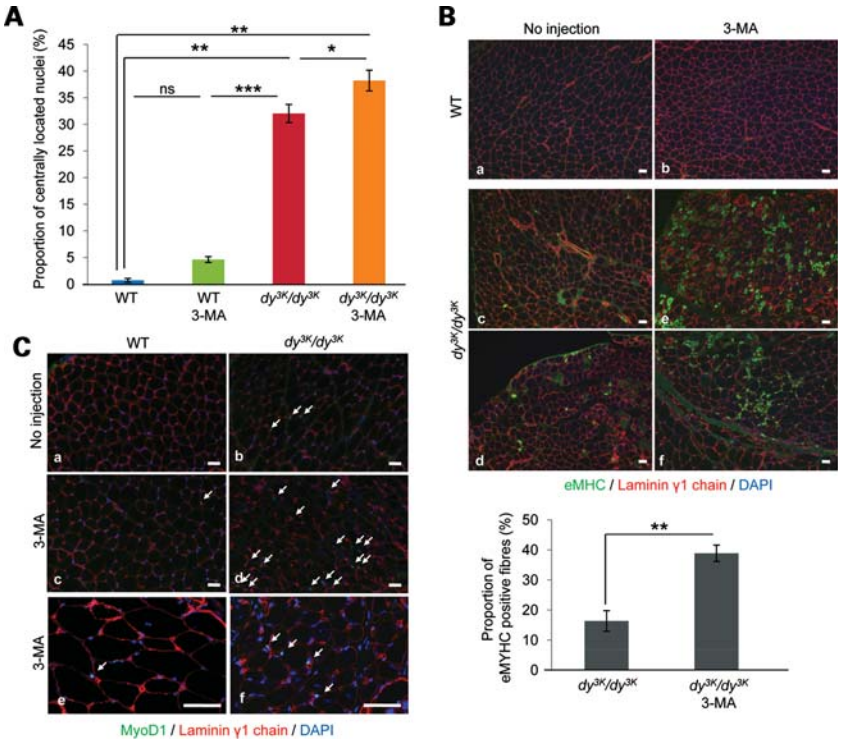

Figure 4. Systemic injection of 3-MA stimulates regeneration in quadriceps muscle of dy^{3K}/dy^{3K} mice. (**A**) Proportion of fibers with centrally located nuclei in 3-MA-injected dy^{3K}/dy^{3K} and wild-type mice, non-injected dy^{3K}/dy^{3K} and wild-type mice ($n = 6$ for each group). (**B,** upper part) Co-immunolabeling on cross-sections of quadriceps muscle from non-injected wild-type ($n = 5$) and dy^{3K}/dy^{3K} ($n = 5$) mice and 3-MA-injected wild-type ($n = 6$) and dy^{3K}/dy^{3K} ($n = 6$) mice. Laminin γ1 chain (red) delineates fiber boundaries and eMHC (green) is expressed only by regenerative cells. DAPI (in blue) denotes nuclei. Bar = 40 μm. (Lower part) Percentage of fibers expressing eMHC. (**C**) Co-immunostaining on cross-sections of quadriceps muscle from non-injected wild-type ($n = 3$) and dy^{3K}/dy^{3K} ($n = 3$) mice and 3-MA-injected wild-type ($n = 4$) and dy^{3K}/dy^{3K} ($n = 4$) mice using antibodies against laminin γ1 chain (red), MyoD (green) and DAPI (blue). Arrows denote MyoD-positive nuclei in the interstitial space between myofibers. The two lower panels (e and f) represent higher magnification of other areas than those shown in (c) and (d). Bar = 40 μm. $^{*}P < 0.05$; $^{**}P < 0.001$.

the same level of activity as wild-type animals (Fig. 7A). Also, 3-MA-treated dy^{3K}/dy^{3K} mice weighed significantly more than non-injected dy^{3K}/dy^{3K} mice, although they never reached the weight of wild-type mice (Fig. 7B). Moreover, the median survival of 3-MA-injected dy^{3K}/dy^{3K} mice was 37 days (Fig. 7C), whereas it has been shown to be 22 days for non-treated dy^{3K}/dy^{3K} mice (16). Finally, although survival and muscle morphology was significantly improved, transient hind leg paralysis often occurred in one leg of 3-MA-treated dy^{3K}/dy^{3K} mice and similar paralysis occurred in non-treated dy^{3K}/dy^{3K} mice but not in 3-MA-injected wild-type mice (16) (data not shown). Yet, this transient paralysis had no evident effect on the locomotive behavior of 3-MA-injected dy^{3K}/dy^{3K} mice. Nevertheless, it is clear that 3-MA did not appreciably improve the pathology of the peripheral nerve. In agreement with this observation, we found no increased mRNA levels of autophagy-related genes in the laminin α2 chain-deficient sciatic nerve (Supplementary Material, Fig. S5).

Combinatorial treatment with 3-MA and the proteasome inhibitor MG-132 does not improve the dystrophic phenotype of dy^{3K}/dy^{3K} mice better than each compound alone

We recently showed that treatment with the proteasome inhibitor MG-132 partially improved the dystrophic dy^{3K}/dy^{3K} phenotype (16). Similar to 3-MA therapy, administration of MG-132 reduced fibrosis, enlarged muscle fiber diameter, reduced apoptosis, restored Akt phosphorylation, enhanced locomotive activity and increased lifespan (16). The only difference among the parameters analyzed was that the 3-MA treatment increased muscle regeneration (Fig. 4), whereas no such effect was seen upon systemic injection of MG-132. Instead, the number of muscle fibers with centrally located nuclei was slightly decreased in MG-132-injected dy^{3K}/dy^{3K} mice (16). To investigate the relative contribution of the proteasome versus the autophagosome in the pathogenesis of MDC1A, we combined 3-MA and MG-132 treatment and assessed whether the effects were additive or not. Combination therapy with 3-MA at 15 mg/kg and MG-132 at 10 mg/kg (as previously used) was not more beneficial than each compound alone. In contrast, muscle morphology was even worse compared with non-treated dy^{3K}/dy^{3K} muscle (data not shown). Therefore, we tested combinatorial therapy with a 10 times lower dose of each drug. Indeed, tenascin-C expression was reduced to near wild-type levels in the double injected dy^{3K}/dy^{3K} mice. However, there was no additional reduction in fibrosis compared with therapy with either drug (Fig. 2B, Supplementary Material, Fig. S6) (16). Double injections with 3-MA and MG-132 also improved locomotion and survival of dy^{3K}/dy^{3K} mice. Yet, there was no added increase in survival compared with treatment with each compound alone (Supplementary Material, Figs S6

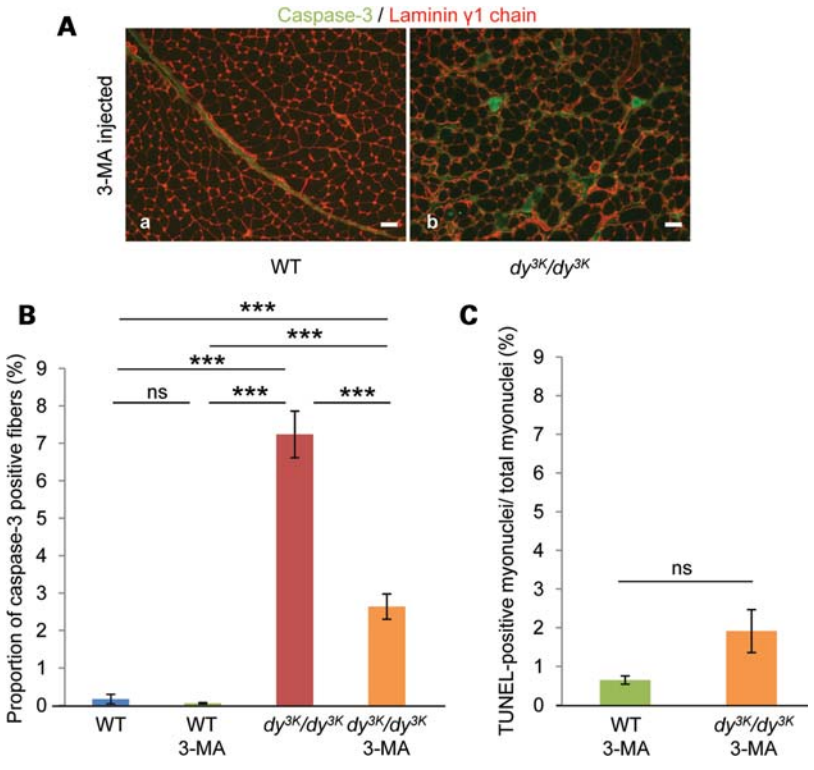

Figure 5. Apoptosis is diminished after systemic injection of 3-MA in dy^{3K}/dy^{3K} mice. (**A**) Co-immunostaining using antibodies against pro-caspase-3 and caspase-3 isoforms (green) and laminin γ1 chain (red) in 3-MA-injected wild-type and dy^{3K}/dy^{3K} quadriceps muscle (a and b). Fourteen days after 3-MA systemic injection, green positive fibers were found in restricted areas of dy^{3K}/dy^{3K} quadriceps muscle, (b) but most parts of the muscle are marked by the absence of apoptotic fibers (a). Bar = 40 μm. (**B**) Percentage of caspase-3-positive fibers in whole quadriceps muscle sections from 3-MA-injected dy^{3K}/dy^{3K} and wild-type mice ($n = 6$ for both). (**C**) Percentage of TUNEL-positive myonuclei in whole quadriceps sections from 3-MA-injected dy^{3K}/dy^{3K} and wild-type mice ($n = 6$ for each group). $^{*}P < 0.05$; $^{***}P < 0.001$.

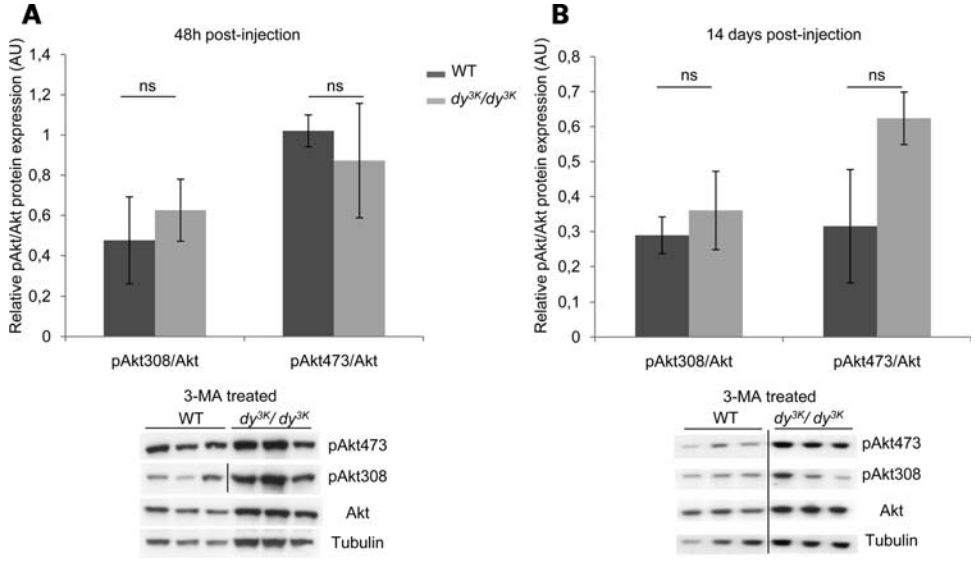

Figure 6. Akt signaling is restored upon autophagy inhibition. Densitometric analysis and representative western blot images of phospho-Akt308/Akt and phospho-Akt473/Akt in quadriceps muscle from 3-MA-injected wild-type and dy^{3K}/dy^{3K} after 48 h (**A**) ($n = 3$ for each genotype) and after 14 days (**B**) ($n =$ 4 and 6, respectively). Data are expressed in arbitrary units (AU) as phospho-Akt was normalized to Akt. Tubulin was used as an internal loading control.

and 7) (16). Moreover, there was no further alteration in the proportion of central nucleation, compared with dy^{3K}/dy^{3K} muscles (Fig. 4A, Supplementary Material, Fig. S6) (16). These data indicate that the ubiquitin–proteasome pathway and the autophagy–lysosome pathway most likely intersect in laminin α2 chain-deficient muscle.

DISCUSSION

MDC1A is a debilitating muscle disease for which there currently is no cure. Several approaches to prevent disease development in MDC1A mouse models have been explored and they include for example gene replacement (28,31,32), anti-apoptosis (20,21), proteasome inhibition (16), cell (33) and improved regeneration therapy (34). While the transgenic strategies (e.g. over-expression of laminin α2 chain, mini-agrin and in particular laminin α1 chain) may have offered the most complete muscle restoration, they are not yet clinically feasible and the pharmacological inhibition of apoptosis and proteasome, respectively, have only resulted in partial recovery. Therefore, new therapeutic options for MDC1A should urgently be explored. Here, we present data indicating that increased autophagy is pathogenic in MDC1A. We found increased expression of several autophagy-related genes in laminin α2 chain-deficient mouse and human muscle. As a proof of concept, we have shown that autophagy inhibition, using 3-MA in the dy^{3K}/dy^{3K} mouse model for MDC1A, significantly reduced many of the pathological symptoms in the dystrophic mice.

Another major feature of MDC1A is apoptosis. It is known that autophagy and apoptosis are interconnected in a very complex manner. Apoptosis and autophagy can act in a coordinated way to induce cell death, or autophagy might counteract or facilitate apoptosis and several regulatory proteins are shared by the two pathways (e.g. mTOR, Atg5 and Bcl-2 proteins) (35–38). Consequently, it would be interesting to test whether the combined inhibition of apoptosis and autophagy would further restore the phenotype of laminin α2 chain-deficient mice. Recent evidence also suggest a crosstalk between the ubiquitin–proteasome pathway and autophagic–lysosomal pathway, as it has been demonstrated that ubiquitinated proteins can be delivered to the autophagosomes through the p62/SQSTM1 complex that is able to bind LC3 (39–43). We also demonstrated that combinatorial treatment of autophagy and proteasome inhibition did not further improve the dy^{3K}/dy^{3K} phenotype, supporting a view that both pathways may be interconnected (at least in laminin α2 chain-deficient muscle).

Interestingly, together with the data we presented here, incorrect function of autophagy has been discovered to be pathogenic in the two most common forms of congenital muscular dystrophy and both are linked to deficiency of extracellular matrix proteins (10). In the collagen VI-deficient mouse model, there is a relative underactivity of the autophagosome (with persistence of structurally abnormal mitochondria) that contributes to the disease process (10). In contrast, absence of laminin α2 chain results in autophagosome overactivity. How does absence of two extracellular matrix proteins result in such contradictory effects on autophagy? Collagen VI is mainly an interstitial matrix protein, although it is closely associated with basement membranes in many organs (44), whereas laminin α2 chain is a basement membrane protein (45). Hence, the two proteins are present in different extracellular matrix structures that may have overlapping but also separate functions in skeletal muscle. Moreover, besides providing support and anchorage for cells, the extracellular matrix also initiates signal transduction pathways (46). Little is known about the laminin α2 chain-induced signaling pathways in skeletal muscle (45) and even less is known about collagen VI-mediated signaling (in skeletal muscle) (47), but it is tempting to speculate that they lead to diverse or even opposite physiological effects. Nevertheless, it is clear that an extracellular matrix unbalance in skeletal muscle affects the autophagy pathway. Also, extracellular matrix abnormalities in epithelial cells induce autophagy (48). The additional data that we provide on the Duchenne mouse model *mdx*, showing that autophagy is not modified when a cytoskeletal protein is missing, reinforce the notion that the extracellular matrix regulates autophagy. Mainly, the expression of lysosomal markers was increased in *mdx* muscle. Hence, in this model, it could be that microautophagy (direct internalization of cytosolic cargo into the lysosome) and/or chaperone-mediated autophagy (degradation of proteins that are recognized by the Hsc70 chaperone and binds Lamp2a) is stimulated with the progression of the disease (3). This should be further clarified as well as the potential primary or secondary contribution of autophagy in other muscular dystrophies associated with defects in extracellular matrix proteins and their receptors. Autophagosomes are present in many myopathies and are the major features of a group of muscle disorders named autophagic vacuolar myopathies. This group is composed by the late-onset Pompe disease caused by a defect in lysosomal acid maltase (MIM ID #232300), the Danon disease that primarily affects the heart due to a defect in the *LAMP2* gene (MIM ID #300257) and the X-linked myopathy with excessive autophagy associated with mutations in the *VMA21* gene (49). Therefore, autophagy-related genes could be mutated in genetically irresolute muscle diseases.

In summary, our study demonstrates for the first time that autophagy can be overactive in a congenital muscular dystrophy condition. In addition, its inhibition improves the muscle phenotype of laminin α2 chain-deficient mice. Thus, we have produced relevant pre-clinical data for the development of pharmacological therapies for MDC1A patients.

MATERIALS AND METHODS

Transgenic animals

Laminin α2 chain-deficient mice (dy^{3K}/dy^{3K}), which completely lack laminin α2 chain, were used and previously described (13,28). These mice develop severe muscular dystrophy and peripheral neuropathy and the median survival is around 22 days (16). For all experiments, dy^{3K}/dy^{3K} mice were compared with their wild-type littermates. Dy^{3K}δE3 mice were also described previously (25). *Mdx* (C57BL/10ScSn-*mdx*/J) and corresponding wild-type mice were obtained from Jackson Laboratory and bred in our animal facility. Animals were maintained in the animal facilities of Biomedical Center (Lund) according to the animal care guidelines, and all mouse experimentation was approved by the Malmö/Lund (Sweden) ethical committee for animal research (permit numbers M62-09 and M122-10).

Primary muscle cell culture and differentiation

Primary myoblasts were obtained from a control fetus (12 weeks of gestation) and a MDC1A fetus (15 weeks of gestation), presenting a homozygous nonsense mutation in exon 31 of the *LAMA2* gene (50). Muscle cells were obtained in accordance

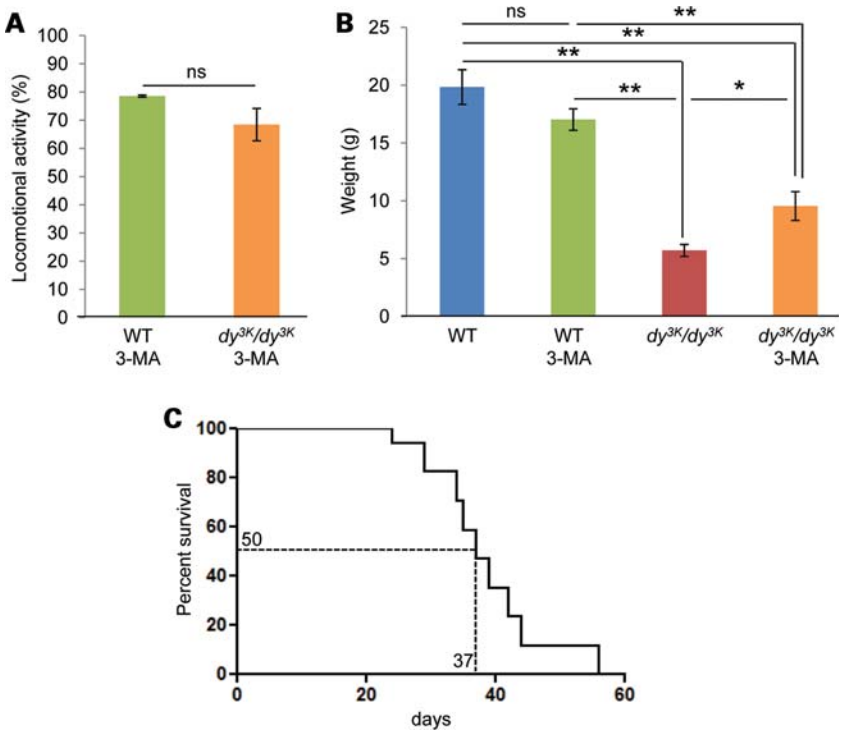

Figure 7. Systemic injection of 3-MA improves dy^{3K}/dy^{3K} mice locomotion, body weight and survival. (**A**) Exploratory locomotion of ~4-week-old mice in an open field test ($n = 14$ for each group). (**B**) Body weight measurement of 4-week-old non-injected and 3-MA-treated wild-type ($n = 7$) and dy^{3K}/dy^{3K} mice ($n = 12$). (**C**) Survival curves of 3-MA-injected dy^{3K}/dy^{3K} mice. The median survival for non-injected dy^{3K}/dy^{3K} mice is 22 days (16), whereas it was 37 days for the treated animals. $^{*}P < 0.05$; $^{**}P < 0.001$.

with the French legislation on ethical rules. Cells were cultivated in six-well plates with growth medium (F10-Ham medium, Gibco) containing 20% fetal bovine serum (Gibco) at 37°C, 5% CO_2. At ~70% confluency, differentiation into myotubes was initiated by switching to fusion medium (Dulbecco's modified eagle's medium, Gibco) containing 2% horse serum (Gibco), 10^{-6} M insulin (Sigma) and 2.5×10^{-6} M dexamethasone (Sigma). Protein lysates were obtained by scraping the cells directly into the lysis buffer (50 mM Tris–HCl, pH 6.8, 10% β-mercaptoethanol, 4% sodium dodecyl sulfate (SDS), 0.03% bromophenol blue and 20% glycerol).

Systemic injections of 3-MA

Systemic administration of 3-MA was performed by intraperitoneal injections [15 mg/kg in sterile phosphate buffered saline (PBS)] into dy^{3K}/dy^{3K} mice and control littermates at the age of 2.5 weeks and 3.5 weeks. Mice were sacrificed 48 h or 14 days after injection and quadriceps, tibialis anterior and diaphragm muscles were processed for morphometric analysis, immunofluorescence experiments, quantitative real-time polymerase chain reaction (qRT–PCR) or western blot analysis. Prior to euthanasia, an exploratory locomotion test was performed (see below).

RNA extraction, reverse transcription and quantitative real-time PCR

Total RNA was extracted from 10 mg of quadriceps muscle from six dy^{3K}/dy^{3K} mice (3.5-week-old) and six wild-type littermates; from three dy^{3K}/dy^{3K} mice (7-day-old) and six wild-type littermates; from three $dy^{3K}\delta$E3 mice (5-week-old) and three wild-type littermates; from five dy^{3K}/dy^{3K} mice and five wild-type littermates treated with 3-MA; from six *mdx* and six wild-type mice (both 5-week-old); from three *mdx* and three wild-type mice (both 3-month-old) and from sciatic nerve from five dy^{3K}/dy^{3K} mice (3.5-week-old) and five wild-type littermates using RNeasy mini kit (Qiagen), including an initial step of proteinase K digestion (Fermentas, 240 ng/μl). Complementary DNA was synthesized from 1 μg of total RNA with random primers and SuperScriptIII reverse transcriptase (Invitrogen) following manufacturer's instructions. Quantitative PCRs were performed in triplicate with the Maxima SYBR Green qPCR Master Mix (Fermentas). Expression of target and reference genes was monitored using a qRT–PCR method (Light Cycler, Roche) with the previously described primers for the autophagic genes *Bnip, Bnip3l, p62*, *LC3B*, *Gabarapl1*, *Atg4b*, *Vps34*, *Beclin*, *Cathepsin L* and *Lamp2a* (8). The amplification efficiency for each primer pair was evaluated by amplification of serially diluted template cDNAs ($E = 10^{-r/slope}$). Efficiency-corrected RNA levels (in arbitrary units) were calculated by using the formula E^{-Ct}. Expression levels were then calculated relative to the endogenous control gene *GAPDH* and relative to wild-type quadriceps.

Protein extraction and western blot analyses

Isolated quadriceps muscles were obtained from six wild-type, six dy^{3K}/dy^{3K} mice (3.5 weeks of age) and six dy^{3K}/dy^{3K} mice

48 h or 14 days after 3-MA injection. Each sample was immediately frozen in liquid nitrogen and reduced to powder using a mortar. Protein extracts were obtained as previously described (16). A total of 30 μg of denaturated proteins was loaded on 10–20% acrylamide SDS gels (Clearpage, CBS Scientific) and blotted onto nitrocellulose membranes (Hybond-C, Amersham) during 1.5 h (Biorad). The membranes were blocked for 1 h at room temperature in PBS, 0.01% Tween 20, 5% milk and incubated overnight at 4°C with rabbit polyclonal antibodies directed against pAkt (Ser 473, 1/2000, #4060 or Thr 308, 1/1000, #2965, Cell Signaling Technology), Akt (1/1000, #4685, Cell Signaling Technology), Vps34 (1/200, V9764, Sigma) or LC3B (1/250, #2775, Cell Signaling Technology). Blots were then washed three times for 10 min with PBS, 0.05% Tween 20, incubated with horseradish peroxidase-conjugated polyclonal goat anti-rabbit (1/4000, sc-2004, Santa Cruz Biotechnology) or goat anti-mouse (1/4000, sc-2005, Santa Cruz Biotechnology) antibody for 1 h. Membranes were incubated in ECL (Amersham Biosciences), exposed on Hyperfilm (Amersham Biosciences) and developed (AGFA, Curix 60). Each membrane was rehybridized with mouse monoclonal anti-tubulin (1/4000, clone DM 1A, Sigma) for loading normalization. The quantifications were performed using ImageJ 1.40 (http://rsb.info.nih.gov/ij/download.html).

Histology and immunofluorescence experiments

Quadriceps (n = at least 6 for each group), tibialis anterior (n = 6, 5, 5 and 8, respectively) and diaphragm (n = 5, 4, 3 and 4, respectively) muscles from wild-type, dy^{3K}/dy^{3K}, 3-MA-injected wild-type and 3-MA-injected dy^{3K}/dy^{3K} mice) were rapidly dissected after euthanasia and frozen in OCT (Tissue Tek) in liquid nitrogen. Serial sections of 7 μm were either stained with hematoxylin and eosin or processed for immunofluorescence experiments following standard procedures (28) with rabbit monoclonal antibody against LC3B (1/100, #3868, Cell Signaling Technology); rabbit polyclonal antibodies against laminin γ1 chain (1/1000, #1083), laminin α4 chain (1/400, #1100) and laminin β2 chain (1/400, #1117) (generously provided by Dr T. Sasaki); rat monoclonal antibodies against laminin γ1 chain (1/200, MAB 1914, Chemicon) and tenascin-C (undiluted, MTn15); goat polyclonal antibody against collagen III (1/100, #1330, SouthernBiotech) and mouse monoclonal antibodies against caspase-3 (1/100, CPP32, BD Transduction Laboratory), eMHC (1/100, F1.652, Developmental Studies Hybridoma Bank) and MyoD (1/100, clone 5.8A, Dako). Human muscle sections, obtained from muscle biopsies from a 2.5-year-old healthy control; two MDC1A patients (2- and 3.5-year-old, respectively) with complete deficiency of laminin α2 chain and from a 21-year-old patient with inclusion-body myositis, were stained with rabbit monoclonal antibody against LC3B (1/100, #3868, Cell Signaling Technology); rabbit polyclonal antibody against LC3B (1/200, #100-2220, Novus Biologicals) and rat monoclonal antibody against perlecan (1/100, MAB 1948, Chemicon). For apoptotic myofiber detection, a TUNEL detection kit was used following instructions of the manufacturer (GenScript). Sections were analyzed using a Zeiss Axioplan fluorescence microscope. Images were captured using an ORCA 1394 ER digital camera with the Openlab 3 software.

Exploratory locomotion test

Exploratory locomotion was examined in an open field test. In each experiment, the mouse 14 days after 3-MA injection (n = 11 for dy^{3K}/dy^{3K} and wild-type, respectively) was placed into a new cage and allowed to explore the cage for 5 min. The time that the mouse spent moving around was measured manually.

Survival curves

Death was monitored in 3-MA-injected dy^{3K}/dy^{3K} mice (n = 9). A survival curve was constructed using the GraphPad Prism 4 software.

Morphometric analysis

Measurements were performed on whole quadriceps, tibialis anterior and diaphragm muscle sections from untreated wild-type and dy^{3K}/dy^{3K} and 3-MA-injected wild-type and dy^{3K}/dy^{3K} animals. Tenascin-C and collagen III-positive areas and fiber diameters were measured and eMHC-positive fibers, caspase-3 positive fibers and TUNEL-positive myonuclei were calculated using the ImageJ software. Minimal Feret's diameter was measured (51) for at least 1500 fibers for each muscle. The same number of fibers was used for quantification of fibers with centrally located nuclei. Wet quadriceps muscle weights were determined from seven non-injected wild-type and dy^{3K}/dy^{3K} and 3-MA-treated wild-type (n = 4) and dy^{3K}/dy^{3K} (n = 6) animals and correlated to body weight.

Combinatorial treatment

Dy^{3K}/dy^{3K} and wild-type littermates were injected intraperitoneally with 3-MA (1.5 mg/kg in sterile PBS) and intravenously with MG-132 (1 μg/kg in sterile PBS) at the age of 2.5 and 3.5 weeks. Mice were sacrificed 14 days after injection and quadriceps muscles were processed for morphometric analysis and immunofluorescence experiments (n = 5 and 4 for each group, respectively). A locomotion test was also performed (n = 9 and 7 for each group, respectively) and survival (n = 4) was monitored.

Statistical analysis

All tests for the analysis of significance were done using the GraphPad Prism 4 software.

For quantitative PCR experiments, protein quantifications, morphometric analysis and exploratory locomotion test, one-way analysis of variance followed by a Bonferroni's post-multiple comparison test was performed. Regarding fiber size distribution, a χ^2-test was calculated and paired comparison of distribution was estimated related for a P-value inferior to 0.0001. Finally, the statistic LogRank test was used for the analysis of significance of survival curves. Data always represent mean ± SEM.

SUPPLEMENTARY MATERIAL

Supplementary Material is available at *HMG* online.

ACKNOWLEDGEMENTS

We are very grateful to Maud Beuvin, Emmanuelle Lacène and Dr Norma B. Romero (UMRS 974 and Myology Insitute, Paris, France) for access to the patients' muscle biopsies. We also would like to thank Mikael Åkerlund for help with mice, Bruno Oliveira for collection of sciatic nerves, Takako Sasaki for providing antibodies and Anne-Cécile Durieux for help and advice regarding western blot experiments.

Conflict of Interest statement. V.C. and M.D. have, together with Lund University Bioscience AB, formed a company with the objective to commercialize the findings comprised in this article.

FUNDING

This work was funded by the Muscular Dystrophy Association, Association Française contre les Myopathies; Crafoord Foundation; Kock Foundation; Marcus Borgström Foundation; Alfred Österlund Foundation; the Royal Physiographic Society and The Swedish Research Council.

REFERENCES

1. Eskelinen, E.L. and Saftig, P. (2009) Autophagy: a lysosomal degradation pathway with a central role in health and disease. *Biochim. Biophys. Acta*, **1793**, 664–673.
2. Kundu, M. and Thompson, C.B. (2008) Autophagy: basic principles and relevance to disease. *Annu. Rev. Pathol.*, **3**, 427–455.
3. Mizushima, N., Levine, B., Cuervo, A.M. and Klionsky, D.J. (2008) Autophagy fights disease through cellular self-digestion. *Nature*, **451**, 1069–1075.
4. Sandri, M. (2010) Autophagy in skeletal muscle. *FEBS Lett.*, **584**, 1411–1416.
5. Masiero, E., Agatea, L., Mammucari, C., Blaauw, B., Loro, E., Komatsu, M., Metzger, D., Reggiani, C., Schiaffino, S. and Sandri, M. (2009) Autophagy is required to maintain muscle mass. *Cell Metab.*, **10**, 507–515.
6. Lum, J.J., DeBerardinis, R.J. and Thompson, C.B. (2005) Autophagy in metazoans: cell survival in the land of plenty. *Nat. Rev. Mol. Cell Biol.*, **6**, 439–448.
7. Mammucari, C., Milan, G., Romanello, V., Masiero, E., Rudolf, R., Del Piccolo, P., Burden, S.J., Di Lisi, R., Sandri, C., Zhao, J. *et al.* (2007) FoxO3 controls autophagy in skeletal muscle *in vivo*. *Cell Metab.*, **6**, 458–471.
8. Zhao, J., Brault, J.J., Schild, A., Cao, P., Sandri, M., Schiaffino, S., Lecker, S.H. and Goldberg, A.L. (2007) FoxO3 coordinately activates protein degradation by the autophagic/lysosomal and proteasomal pathways in atrophying muscle cells. *Cell Metab.*, **6**, 472–483.
9. Zhao, J., Brault, J.J., Schild, A. and Goldberg, A.L. (2008) Coordinate activation of autophagy and the proteasome pathway by FoxO transcription factor. *Autophagy*, **4**, 378–380.
10. Grumati, P., Coletto, L., Sabatelli, P., Cescon, M., Angelin, A., Bertaggia, E., Blaauw, B., Urciuolo, A., Tiepolo, T., Merlini, L. *et al.* (2010) Autophagy is defective in collagen VI muscular dystrophies, and its reactivation rescues myofiber degeneration. *Nat. Med.*, **16**, 1313–1320.
11. Voit, T. and Tome, F.M. (2004) The congenital muscular dystrophies. In Engel, A.G. and Franzini-Armstrong, C. (eds), *Myology*, vol. II, 3rd edn. McGrawHill, pp. 1203–1238.
12. Tome, F.M., Evangelista, T., Leclerc, A., Sunada, Y., Manole, E., Estournet, B., Barois, A., Campbell, K.P. and Fardeau, M. (1994) Congenital muscular dystrophy with merosin deficiency. *C. R. Acad. Sci. III*, **317**, 351–357.
13. Miyagoe, Y., Hanaoka, K., Nonaka, I., Hayasaka, M., Nabeshima, Y., Arahata, K. and Takeda, S. (1997) Laminin α2 chain-null mutant mice by targeted disruption of the Lama2 gene: a new model of merosin (laminin 2)-deficient congenital muscular dystrophy. *FEBS Lett.*, **415**, 33–39.
14. Nakagawa, M., Miyagoe-Suzuki, Y., Ikezoe, K., Miyata, Y., Nonaka, I., Harii, K. and Takeda, S. (2001) Schwann cell myelination occurred without basal lamina formation in laminin alpha2 chain-null mutant (dy^{3K}/dy^{3K}) mice. *Glia*, **35**, 101–110.
15. Allamand, V. and Guicheney, P. (2002) Merosin-deficient congenital muscular dystrophy, autosomal recessive (MDC1A, MIM#156225, LAMA2 gene coding for α2 chain of laminin). *Eur. J. Hum. Genet.*, **10**, 91–94.
16. Carmignac, V., Quere, R. and Durbeej, M. (2011) Proteasome inhibition improves the muscle of laminin α2 chain-deficient mice. *Hum. Mol. Genet.*, **20**, 541–552.
17. Vachon, P.H., Xu, H., Liu, L., Loechel, F., Hayashi, Y., Arahata, K., Reed, J.C., Wewer, U.M. and Engvall, E. (1997) Integrins (α7β1) in muscle function and survival. Disrupted expression in merosin-deficient congenital muscular dystrophy. *J. Clin. Invest.*, **100**, 1870–1881.
18. Hayashi, Y.K., Tezak, Z., Momoi, T., Nonaka, I., Garcia, C.A., Hoffman, E.P. and Arahata, K. (2001) Massive muscle cell degeneration in the early stage of merosin-deficient congenital muscular dystrophy. *Neuromuscul. Disord.*, **11**, 350–359.
19. Dominov, J.A., Kravetz, A.J., Ardelt, M., Kostek, C.A., Beermann, M.L. and Miller, J.B. (2005) Muscle-specific BCL2 expression ameliorates muscle disease in laminin α2-deficient, but not in dystrophin-deficient, mice. *Hum. Mol. Genet.*, **14**, 1029–1040.
20. Girgenrath, M., Dominov, J.A., Kostek, C.A. and Miller, J.B. (2004) Inhibition of apoptosis improves outcome in a model of congenital muscular dystrophy. *J. Clin. Invest.*, **114**, 1635–1639.
21. Erb, M., Meinen, S., Barzaghi, P., Sumanovski, L.T., Courdier-Fruh, I., Ruegg, M.A. and Meier, T. (2009) Omigapil ameliorates the pathology of muscle dystrophy caused by laminin-α2 deficiency. *J. Pharmacol. Exp. Ther.*, **331**, 787–795.
22. Girgenrath, M., Beermann, M.L., Vishnudas, V.K., Homma, S. and Miller, J.B. (2009) Pathology is alleviated by doxycycline in a laminin-α2-null model of congenital muscular dystrophy. *Ann. Neurol.*, **65**, 47–56.
23. Levine, B. and Kroemer, G. (2008) Autophagy in the pathogenesis of disease. *Cell*, **132**, 27–42.
24. Maiuri, M.C., Zalckvar, E., Kimchi, A. and Kroemer, G. (2007) Self-eating and self-killing: crosstalk between autophagy and apoptosis. *Nat. Rev. Mol. Cell Biol.*, **8**, 741–752.
25. Gawlik, K.I., Åkerlund, M., Carmignac, V., Elamaa, H. and Durbeej, M. (2010) Distinct roles for laminin globular domains in laminin α1 chain mediated rescue of murine laminin α2 chain deficiency. *PLoS ONE*, **5**, e11549.
26. Barresi, R. and Campbell, K.P. (2006) Dystroglycan: from biosynthesis to pathogenesis of human disease. *J. Cell Sci.*, **119**, 199–207.
27. Ravikumar, B., Sarkar, S., Davies, J.E., Futter, M., Garcia-Arencibia, M., Green-Thompson, Z.W., Jimenez-Sanchez, M., Korolchuk, V.I., Lichtenberg, M., Luo, S. *et al.* (2010) Regulation of mammalian autophagy in physiology and pathophysiology. *Physiol. Rev.*, **90**, 1383–1435.
28. Gawlik, K., Miyagoe-Suzuki, Y., Ekblom, P., Takeda, S. and Durbeej, M. (2004) Laminin α1 chain reduces muscular dystrophy in laminin α2 chain deficient mice. *Hum. Mol. Genet.*, **13**, 1775–1784.
29. Cohn, R.D., Herrmann, R., Wewer, U.M. and Voit, T. (1997) Changes of laminin β2 chain expression in congenital muscular dystrophy. *Neuromuscul. Disord.*, **7**, 373–378.
30. Bentzinger, C.F., Barzaghi, P., Lin, S. and Ruegg, M.A. (2005) Overexpression of mini-agrin in skeletal muscle increases muscle integrity and regenerative capacity in laminin-α2-deficient mice. *FASEB J.*, **19**, 934–942.
31. Kuang, W., Xu, H., Vachon, P.H., Liu, L., Loechel, F., Wewer, U.M. and Engvall, E. (1998) Merosin-deficient congenital muscular dystrophy. Partial genetic correction in two mouse models. *J. Clin. Invest.*, **102**, 844–852.
32. Meinen, S., Barzaghi, P., Lin, S., Lochmuller, H. and Ruegg, M.A. (2007) Linker molecules between laminins and dystroglycan ameliorate

laminin-α2-deficient muscular dystrophy at all disease stages. *J. Cell Biol.*, **176**, 979–993.
33. Hagiwara, H., Ohsawa, Y., Asakura, S., Murakami, T., Teshima, T. and Sunada, Y. (2006) Bone marrow transplantation improves outcome in a mouse model of congenital muscular dystrophy. *FEBS Lett.*, **580**, 4463–4468.
34. Kumar, A., Yamauchi, J., Girgenrath, T. and Girgenrath, M. (2011) Muscle-specific expression of insulin-like growth factor 1 improves outcome in Lama2Dy-w mice, a model for congenital muscular dystrophy type 1A. *Hum. Mol. Genet.*, **20**, 2333–2343.
35. Mammucari, C., Schiaffino, S. and Sandri, M. (2008) Downstream of Akt: FoxO3 and mTOR in the regulation of autophagy in skeletal muscle. *Autophagy*, **4**, 524–526.
36. Pattingre, S., Tassa, A., Qu, X., Garuti, R., Liang, X.H., Mizushima, N., Packer, M., Schneider, M.D. and Levine, B. (2005) Bcl-2 antiapoptotic proteins inhibit Beclin 1-dependent autophagy. *Cell*, **122**, 927–939.
37. Scott, R.C., Juhasz, G. and Neufeld, T.P. (2007) Direct induction of autophagy by Atg1 inhibits cell growth and induces apoptotic cell death. *Curr. Biol.*, **17**, 1–11.
38. Eisenberg-Lerner, A., Bialik, S., Simon, H.U. and Kimchi, A. (2009) Life and death partners: apoptosis, autophagy and the cross-talk between them. *Cell Death Differ.*, **16**, 966–975.
39. Ichimura, Y., Kominami, E., Tanaka, K. and Komatsu, M. (2008) Selective turnover of p62/A170/SQSTM1 by autophagy. *Autophagy*, **4**, 1063–1066.
40. Ichimura, Y., Kumanomidou, T., Sou, Y.S., Mizushima, T., Ezaki, J., Ueno, T., Kominami, E., Yamane, T., Tanaka, K. and Komatsu, M. (2008) Structural basis for sorting mechanism of p62 in selective autophagy. *J. Biol. Chem.*, **283**, 22847–22857.
41. Kirkin, V., McEwan, D.G., Novak, I. and Dikic, I. (2009) A role for ubiquitin in selective autophagy. *Mol. Cell*, **34**, 259–269.
42. Komatsu, M., Waguri, S., Koike, M., Sou, Y.S., Ueno, T., Hara, T., Mizushima, N., Iwata, J., Ezaki, J., Murata, S. *et al.* (2007) Homeostatic levels of p62 control cytoplasmic inclusion body formation in autophagy-deficient mice. *Cell*, **131**, 1149–1163.
43. Pankiv, S., Clausen, T.H., Lamark, T., Brech, A., Bruun, J.A., Outzen, H., Overvatn, A., Bjorkoy, G. and Johansen, T. (2007) p62/SQSTM1 binds directly to Atg8/LC3 to facilitate degradation of ubiquitinated protein aggregates by autophagy. *J. Biol. Chem.*, **282**, 24131–24145.
44. Groulx, J.F., Gagné, D., Benoit, Y.D., Martel, D., Basora, N. and Beaulieu, J.F. (2011) Collagen VI is a basement protein that regulates epithelial cell-fibronectin interactions. *Matrix Biol.*, **3**, 195–206.
45. Gawlik, K.I. and Durbeej, M. (2011) Skeletal muscle laminin and MDC1A: pathogenesis and treatment strategies. *Skeletal Muscle*, **1**, 9.
46. Bruckner, P. (2010) Suprastructures of extracellular matrices: paradigms of functions controlled by aggregates rather than molecules. *Cell Tissue Res.*, **339**, 7–18.
47. Collins, J. and Bönnemann, C.G. (2010) Congenital muscular dystrophies: toward molecular therapeutic inventions. *Curr. Neurol. Neurosci. Rep.*, **2**, 83–91.
48. Lock, R. and Debnath, J. (2008) Extracellular matrix regulation of autophagy. *Curr. Opin. Cell Biol.*, **5**, 583–588.
49. Ramachandran, N., Munteanu, I., Wang, P., Aubourg, P., Rilstone, J.J., Israelian, N., Naranian, T., Paroutis, P., Guo, R., Ren, Z.P. *et al.* (2009) VMA21 deficiency causes an autophagic myopathy by compromising V-ATPase activity and lysosomal acidification. *Cell*, **137**, 235–246.
50. Allamand, V., Bidou, L., Arakawa, M., Floquet, C., Shiozuka, M., Paturneau-Jouas, M., Gartioux, C., Butler-Browne, G.S., Mouly, V., Rousset, J.P. *et al.* (2008) Drug-induced readthrough of premature stop codons leads to the stabilization of laminin α2 chain mRNA in CMD myotubes. *J. Gene Med.*, **10**, 217–224.
51. Briguet, A., Courdier-Fruh, I., Foster, M., Meier, T. and Magyar, J.P. (2004) Histological parameters for the quantitative assessment of muscular dystrophy in the *mdx*-mouse. *Neuromuscul. Disord.*, **14**, 675–682.